analytical chemistry

ARTICLE

pubs.acs.org/ac

Degradation Process of Lead Chromate in Paintings by Vincent van Gogh Studied by Means of Synchrotron X-ray Spectromicroscopy and Related Methods. 2. Original Paint Layer Samples

Letizia Monico,[†,‡] Geert Van der Snickt,[‡] Koen Janssens,[‡,*] Wout De Nolf,[‡] Costanza Miliani,[§] Joris Dik,[⊥] Marie Radepont,[‡,¶] Ella Hendriks,[△] Muriel Geldof,[◆] and Marine Cotte[¶,#]

[†]Dipartimento di Chimica, Università degli Studi di Perugia, via Elce di Sotto 8, I-06123 Perugia, Italy

[‡]Department of Chemistry, University of Antwerp, Universiteitsplein 1, B-2610 Wilrijk, Belgium

[§]Istituto CNR di Scienze e Tecnologie Molecolari (CNR-ISTM), c/o Dipartimento di Chimica, Università degli Studi di Perugia, via Elce di Sotto 8, I-06123 Perugia, Italy

[⊥]Department of Materials Science and Engineering, Delft University of Technology, Mekelweg 2, NL-2628CD Delft, The Netherlands

[¶]Centre de Recherche et de Restauration des Musées de France, CNRS UMR171, Palais du Louvre, Porte des Lions, 14 Quai François Mitterrand, F-75001 Paris, France

[△]Van Gogh Museum, Paulus Potterstraat 7, 1070 AJ Amsterdam, The Netherlands

[◆]The Netherlands Cultural Heritage Agency (RCE), Movable Heritage Knowledge Sector, Hobbemastraat 22, 1071 ZC Amsterdam, The Netherlands

[#]European Synchrotron Radiation Facility, Polygone Scientifique Louis Néel -6, rue Jules Horowitz - F-38000 Grenoble, France

ABSTRACT: The darkening of the original yellow areas painted with the chrome yellow pigment ($PbCrO_4$, $PbCrO_4 \cdot xPbSO_4$, or $PbCrO_4 \cdot xPbO$) is a phenomenon widely observed on several paintings by Vincent van Gogh, such as the famous different versions of *Sunflowers*. During our previous investigations on artificially aged model samples of lead chromate, we established for the first time that darkening of chrome yellow is caused by reduction of $PbCrO_4$ to $Cr_2O_3 \cdot 2H_2O$ (viridian green), likely accompanied by the presence of another Cr(III) compound, such as either $Cr_2(SO_4)_3 \cdot H_2O$ or $(CH_3CO_2)_7Cr_3(OH)_2$ [chromium(III) acetate hydroxide]. In the second part of this work, in order to demonstrate that this reduction phenomenon effectively takes place in real paintings, we study original paint samples from two paintings of V. van Gogh. As with the model samples, in view of the thin superficial alteration layers that are present, high lateral resolution spectroscopic methods that make use of synchrotron radiation (SR), such as microscopic X-ray absorption near edge (μ-XANES) and X-ray fluorescence spectrometry (μ-XRF) were employed. Additionally, μ-Raman and mid-FTIR analyses were carried out to completely characterize the samples. On both paint microsamples, the local presence of reduced Cr was demonstrated by means of μ-XANES point measurements. The presence of Cr(III) was revealed in specific areas, in some cases correlated to the presence of Ba(sulfate) and/or to that of aluminum silicate compounds.

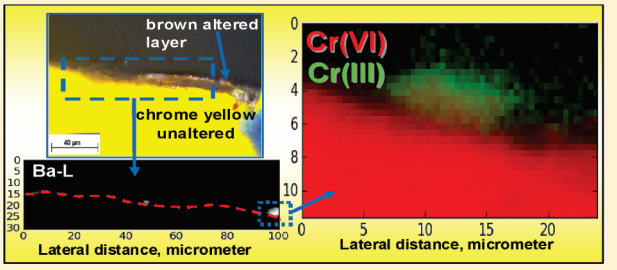

The alteration of chrome yellow ($PbCrO_4$, $PbCrO_4 \cdot xPbSO_4$, or $PbCrO_4 \cdot xPbO$),[1,2] a bright yellow pigment used in both industrial and artistic paints, is a well-known phenomenon which has been studied continuously since its invention in the first decades of the 19th Century. Chrome yellow was often used by artists of the end of 19th Century,[3−8] and also by Vincent van Gogh (1853−1890).[9] In general, on many of these paintings, more than one Century after their creation the areas painted with chrome yellow appear darkened, likely due to a degradation of the pigment itself. Among these paintings the most famous are the different versions of *Sunflowers* by V. van Gogh.

Systematic studies about the degradation mechanisms of lead chromates were carried out until ca. 1950[10−13] [date coinciding with the introduction of stabilized lead chromates and lead molybdates,[1,10,14] and the progressive replacement of chrome yellow with other new synthetic yellow pigments, such as CdS, which was assumed to be more stable[15,16]], and all of them agree that this degradation involves a reduction reaction of Cr(VI) to Cr(III).

However, neither detailed information about the exact mechanism of alteration of $PbCrO_4$ nor about the characterization of the degradation products are provided. Very recently, the darkening of the pigment zinc potassium chromate has been attributed by Casadio et al.[17] to both the chromate−dichromate equilibrium and to a slight reduction of the chromate, leading to the formation of Cr(III) oxide species.

The physical−chemical properties and the factors that may affect the stability of chrome yellow are described in detail in the part 1 of this work.[18] In this study, conducted on artificially aged model samples of lead chromate by means of SR μ-XANES, SR μ-XRF,

Received: September 22, 2010
Accepted: December 15, 2010

   dx.doi.org/10.1021/ac1025122 | *Anal. Chem.* XXXX, XXX, 000–000

Figure 1. Photographs of (top) *Banks of the Seine* (F 293 s 77 v/1962), mid May to mid July 1887, oil on canvas (32 x 46 cm), and (bottom) *View of Arles with Irises* (F 409 s 37 v/1962), May 1888, oil on canvas (54 x 65 cm), by Vincent van Gogh, Van Gogh Museum (Vincent van Gogh foundation), Amsterdam.

and electron energy loss spectrometry (EELS), we were able to establish for the first time that darkening of chromate yellow is caused by a substantial, superficial reduction of the original Cr(VI) to Cr(III). Particularly, $PbCrO_4$ degrades to give $Cr_2O_3 \cdot 2H_2O$ (viridian green), likely accompanied by the presence of another Cr(III) compound, such as either $Cr_2(SO_4)_3 \cdot H_2O$ or $(CH_3CO_2)_7Cr_3(OH)_2$ [chromium(III) acetate hydroxide]. Moreover, this Cr(III) species was especially formed in a thin superficial layer of ca. 1−2 μm thickness.

In what follows, in continuity with the first part of this work[18] and considering the capability of synchrotron X-ray techniques in detecting with extreme sensitivity the distribution of specific species of a given chemical element, μ-XANES and μ-XRF spectrometry were employed to study two embedded paint cross sections, where alteration of the chrome yellow may have taken place, taken from paintings by Vincent Van Gogh from the collection of the Van Gogh Museum (VGM), Amsterdam (Figure 1). Additionally, μ-Raman and μ-FTIR spectroscopy were employed in order to obtain a complete characterization of these microsamples.

EXPERIMENTAL SECTION

Materials. *Original Paint Samples.* Conservators of the VGM, in collaboration with researchers of the ICN/RCE supplied cross sections of paint samples from altered lead chromate areas of two paintings by Vincent van Gogh: *Banks of the Seine* (F293), 1887, and *View of Arles with Irises* (F409), 1888 (Figure 1). The samples were taken during earlier studies resp. by E. Hendriks, VGM, in an area of painting F293 with yellow impasto brushwork, covered by discolored varnish and by M. De Wild, TUDelft in a yellow area of the field shown in painting F409. The samples were kept under darkness until the investigation. They were embedded in polyester resin (Poly-pol, Poly-service, Amsterdam, NL) and ground with Micro-Mesh sheets (Wilton, Iowa, USA) prior to inspection by polarized light and electron microscopy.

Methods. Similar to what has been done previously for the artificially aged model samples, after a preliminary characterization of the original paint samples (by μ-Raman and μ-FTIR spectroscopy in reflection mode), high resolution SR μ-XRF maps were collected on selected areas to identify and better document the elemental composition of paint layers and establish the presence of optional degradation products. Moreover, SR μ-XANES analyses at the Cr K-edge were performed on selected areas of each paint sample. In some cases, the resulting spectral distributions were compared to references in order to obtain information about the Cr oxidation state. The XANES spectra were fitted as linear combination of a limited set of Cr-reference compound spectra in order to semiquantitatively determine the Cr-speciation.

μ-Raman spectra were recorded using a JASCO Ventuno double-grating spectrophotometer equipped with a charge-coupled device (CCD) detector cooled to −50 °C and coupled to an optical microscope (Olympus). Raman spectra were excited using green radiation (532 nm) from an Nd:YAG laser. The laser power used to irradiate the samples was kept between 1 and 2 mW; the exposure time varied between 10 and 20 s with five accumulations. The spectral resolution was about 2 cm^{-1}. Calibration of the spectrometer was performed using the Raman lines of two standards: polystyrene and sulfur.

The instrument used to carry out μ-FTIR analysis consists of a JASCO FTIR 4100 spectrometer, equipped with a 16-channel linear array MCT detector and an IRT-7000 optical microscope. Measurements were performed in reflection mode (through a Cassegrain 16X objective) in an energy range of 6000−600 cm^{-1} and at a resolution of 4 cm^{-1}. The spectra were recorded using 800 scans; background correction was performed by means of a spectrum collected from an aluminum plate.

μ-XRF and μ-XANES analyses were performed at the European Synchrotron Radiation Facility (ESRF, Grenoble, France) using beamline ID21. This instrument operates in the primary energy range from 2.1 to 7.2 keV. A Si(220) fixed-exit double-crystal monochromator was used to produce a highly monochromatic primary beam ($\Delta E/E = 10^{-4}$).

μ-XRF and μ-XANES experiments were carried out in vacuum (10^{-6} mbar), in order (i) to minimize air absorption (which is significant for light elements and for low-energy X-ray fluorescence lines), (ii) to avoid contributions to the spectral background due to scattering in air, and (iii) to prevent sample contamination. A focused beam of ca. 0.95 × 0.25 μm^2 (horizontal × vertical), obtained by means of a Fresnel zone plate, was used for sample irradiation. During the μ-XANES energy scans, the position of the primary beam was maintained stable within 0.5 μm. The procedure employed for correction of the beam spot motion during energy scans is explained elsewhere.[19] The μ-XRF signals were collected in the horizontal plane and perpendicular to the primary beam by means of an HPGe solid-state energy-dispersive detector.

dx.doi.org/10.1021/ac1025122 |*Anal. Chem.* XXXX, XXX, 000–000

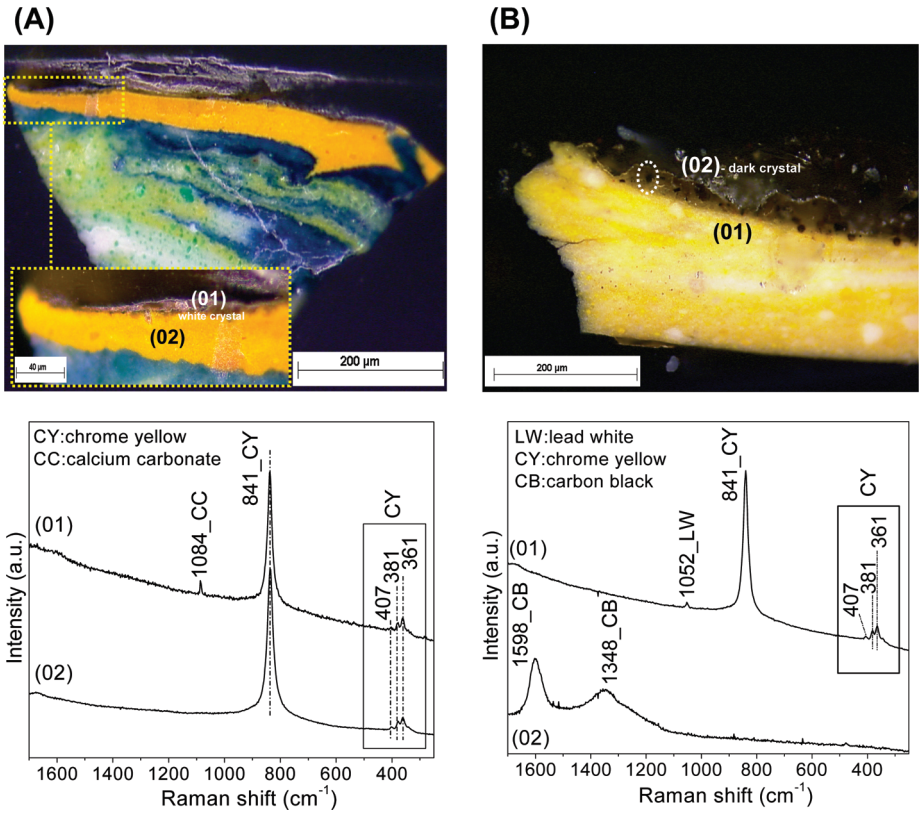

Figure 2. Visible light microscopy image (top) and Raman spectra (bottom) for van Gogh painting samples F409 (panel A) and F293 (panel B). Measuring positions are indicated on the pictures. Panel A: (01) white crystal on brown layer (chrome yellow and calcium carbonate); (02) yellow area (chrome yellow). Panel B: (01) white-yellow area (lead white, chrome yellow); (02) black grain on brown layer (carbon black). Laser power 1 mW, λ = 532 nm, exposure time 20 s, five accumulations.

Table 1. Original Paint Layer Samples: Origin, Colour and Thickness of Layers, μ-Raman, and μ-FTIR Reflection Results

sample name	origin of paint sample	layer color and thickness	μ-Raman	μ-FTIR
F293	*Banks of the Seine*, 1887, (VGM)	brown, 50 μm	carbon black (black grains), lead chromate	aluminum silicate compounds
		yellow, white, 150 μm	lead chromate, lead white	lead white[a]
F409	*View of Arles with Irises*, 1888, (VGM)	brown, 10 μm	lead chromate and calcium carbonate (white grains)	calcium carbonate, aluminum silicate compounds, sulfates
		yellow, 60 μm	lead chromate	lead chromate
		white, yellow, blue, 250 μm	lead white, lead chromate, emerald green (green-blue grains), Prussian blue	lead white, Prussian blue, emerald green

[a] Difficulties in attributing the signals of lead chromate by μ-FTIR because it is present in small amounts compared to the abundantly present lead white.

This device is characterized by a resolution of 130 eV at 6 keV; the detection limit for elements with atomic number between P and Fe typically is around 10 ppm. The sample surface was oriented vertically and at an angle of 60° relative to the incident beam. Both the setup and the procedure for evaluation of XRF spectra are described in greater detail elsewhere.[20] During the μ-XRF mapping experiments, the fluorescence signals were generated by employing a monochromatic primary beam of fixed energy (around 5.989 keV at the Cr K-edge). To compensate for incident beam intensity variations, a normalization detector (I_0) is located just upstream of the sample. The program PyMca was used to fit fluorescence spectra and to separate the different elemental contributions. In the present context, it was in particular crucial to distinguish the partially overlapping Pb−M lines and S−K lines. This program was employed as a batch fitting procedure on each pixel of two-dimensional (2D) maps.[21]

μ-XANES spectra were acquired by scanning the primary energy around the Cr K-edge (5.96−6.09 keV) with a step size of 0.2 eV. The energy calibration was performed using a metallic Cr foil. For all XANES spectra, the procedure of normalization was performed by means of ATHENA, a software program widely used for (E)XA(F)S data analysis. In particular, edge-step normalization of the data was performed by means of linear pre-edge subtraction and by regression of a quadratic polynomial beyond the edge.[22] The same software was also used to carry out a linear combinatorial fitting of XANES spectra of unknown mixtures of Cr-species against a library of XANES spectra of pure Cr-reference compounds. During this procedure, ATHENA attempts to find the best fit between the XANES spectra of the unknown mixtures using a large number of different combinations of the available reference spectra.

dx.doi.org/10.1021/ac1025122 |*Anal. Chem.* XXXX, XXX, 000–000

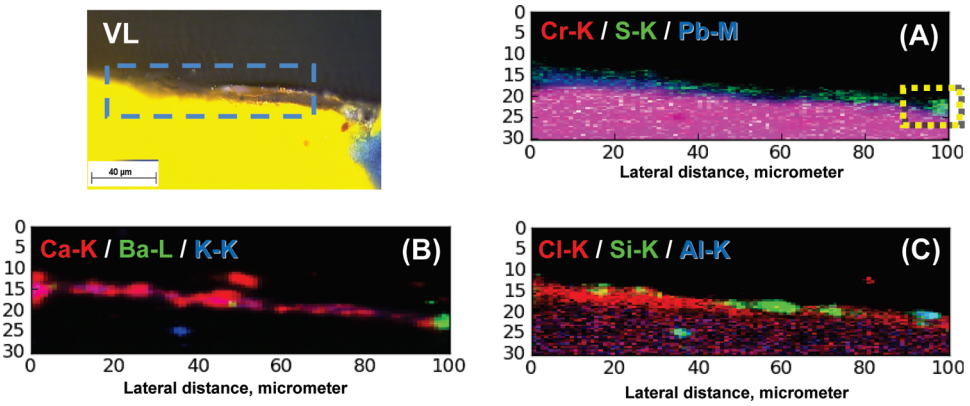

Figure 3. Visible light microscopy image (VL) and RGB composite images of Cr/S/Pb (panel A), Ca/Ba/K (panel B), and Cl/Si/Al (panel C) of paint sample F409 (obtained by μ-XRF at a primary beam energy of 6.086 keV). Map size: 30 × 100 μm^2; pixel size: 0.4 × 1 μm^2; dwell time: 0.3 s. In panel A, the yellow rectangle indicates the region in which more detailed XANES analyses were performed (see Figure 5).

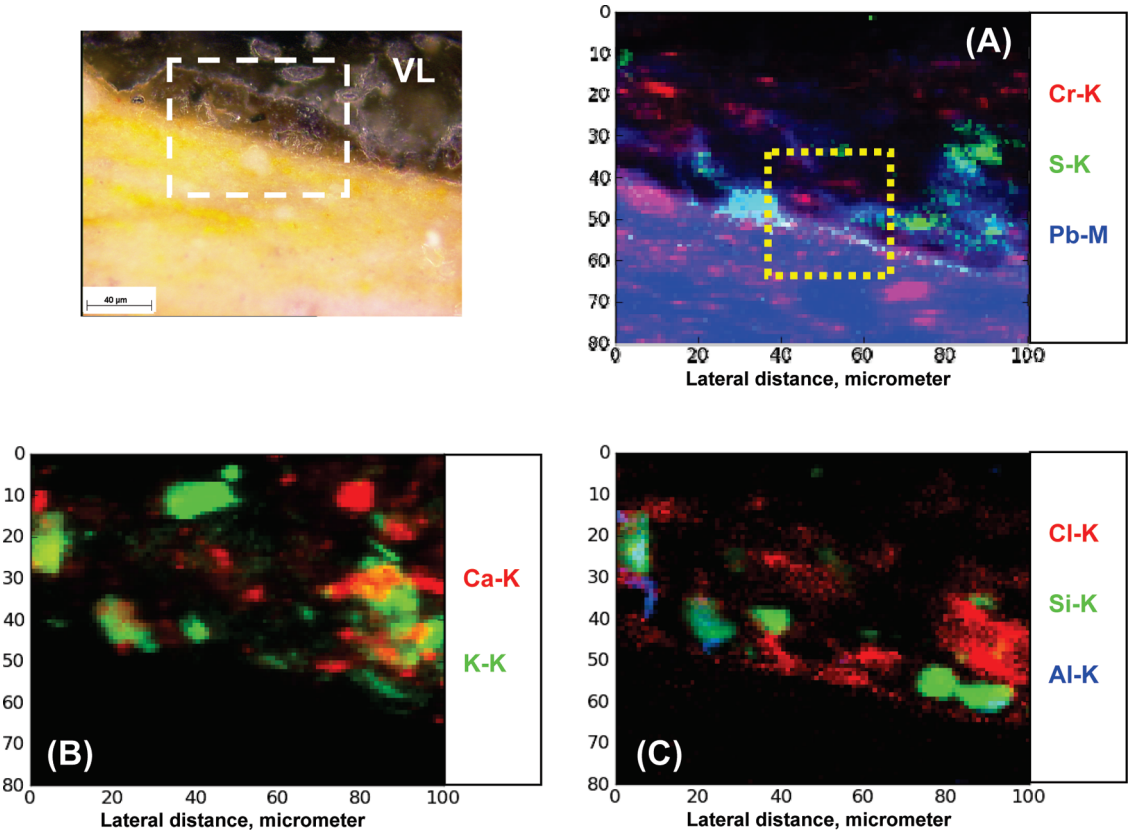

Figure 4. Visible light microscopy image (VL) and RGB composite images of Cr/S/Pb (panel A), Ca/K (panel B), and Cl/Si/Al (panel C) of paint sample F293 (obtained by μ-XRF at a primary beam energy of 6.086 keV). Map size: 80 × 100 μm^2; pixel size: 1 × 1 μm^2; dwell time: 0.3 s. In panel A, the yellow rectangle indicates the region in which more detailed XANES analyses were performed (see Figure 6).

RESULTS AND DISCUSSION

Original Paint Layer Samples. *Optical and Microscopic Observations and Pigment Characterization.* The optical micrographs of embedded and cross-sectioned paint samples F409 (Figure 2A) and F293 (Figure 2B) reveal in both cases the presence of a dark layer at the exposed surface in direct contact with a bright yellow paint layer. This decoloration could be attributed to the degradation or soiling of the yellow paint itself and/or of organic material (such as a varnish or a resin wax) that was applied on the surface in the past. Sample F409 is characterized by a stratigraphy more complex than that of sample F293. In the former sample, the yellow paint layer, present between the brown alteration layer and a blue-white-yellow layer, also contains some green-blue grains. In sample F293 sample, only two layers can be observed: the superficial dark brown layer (containing some black grains) and an inhomogeneous mixture of a yellow and white paint in the layer underneath.

The results of the preliminary characterization of these samples by means of μ-Raman spectroscopy and μ-FTIR reflection analysis are summarized in Table 1.

dx.doi.org/10.1021/ac1025122 |*Anal. Chem.* XXXX, XXX, 000–000

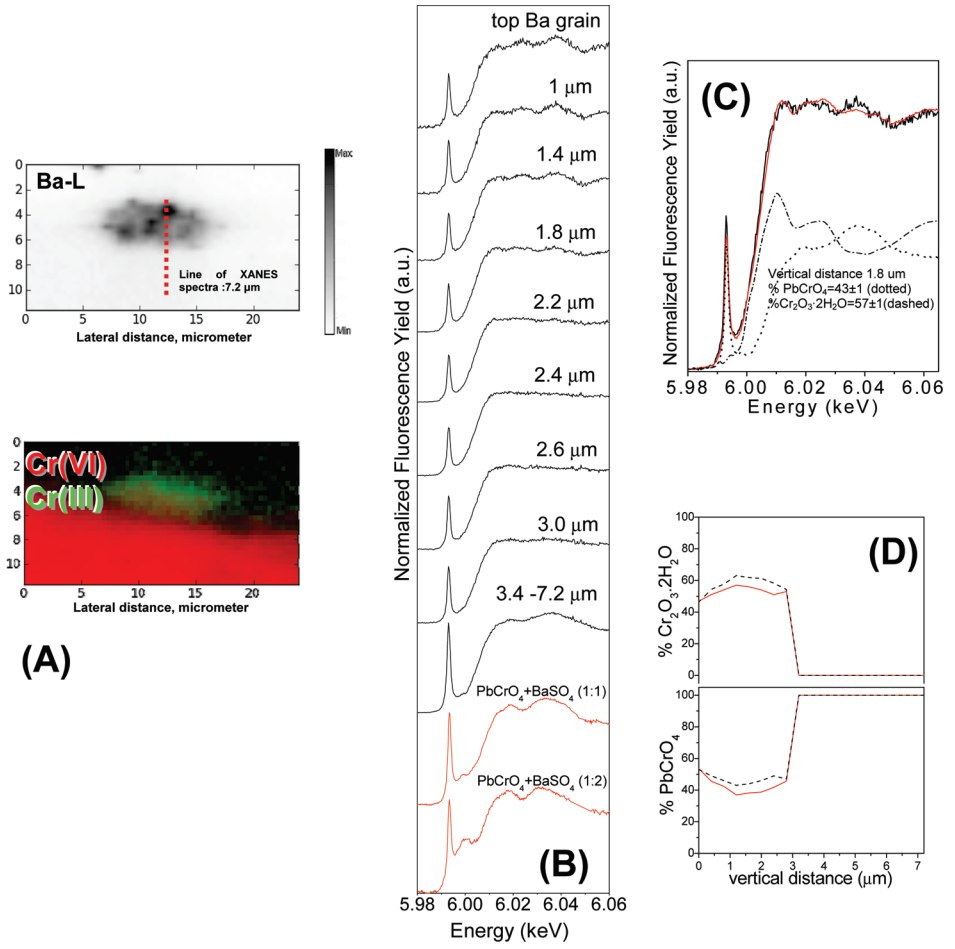

Figure 5. Panel A: Ba distribution (top) and RG composite image of Cr(VI) and Cr(III) maps (bottom) obtained by μ-XRF of paint sample F409. Map size: 11.6 × 24 μm^2; pixel size: 0.4 × 0.4 μm^2; dwell time: 0.3 s. The mapped area is shown in Figure 3A, indicated by a yellow rectangle. Panel B: Cr K-edge XANES line scan (of step size 0.4 μm) recorded through the middle of the Ba-, S-rich grain. The spectra acquired between the top of the Ba grain and 3 μm correspond to a Cr-, Ba-, S-rich area inside the brown layer; those recorded between 3.4 and 7.2 μm correspond to Cr-rich areas inside the yellow layer. In red, at the bottom, Cr−K edge XANES spectra of "$PbCrO_4$/$BaSO_4$" reference compound mixtures in different weight percentages. Panel C: Computation on one of the μ-XANES spectra at the Cr K-edge (recorded at vertical distance = 1.2 μm). (Red) Fit of the experimental data (black) by combination of $PbCrO_4$ (dotted) and $Cr_2O_3 \cdot 2H_2O$ (dashed) and relative result obtained. Panel D: comparison between the % relative abundances of $Cr_2O_3 \cdot 2H_2O$ (top) and $PbCrO_4$ (bottom) obtained from the linear combination procedure (red) and from the analysis of normalized chemical state μ-XRF maps of Cr(III) and Cr(VI) shown in Figure 5 (dashed).

For sample F409, Raman analysis (Figure 2A) shows that the yellow area is composed of chrome yellow [$PbCrO_4$, signals at 841 (CrO_4^{2-} symmetric stretching), 407, 381, and 361 cm^{-1} (CrO_4^{2-} bending modes)].[23] For sample F293 (Figure 2B) in the yellow-white areas, a mixture of lead white [$2PbCO_3 \cdot Pb(OH)_2$ (identified by a band at 1052 cm^{-1}, CO_3^{2-} symmetric stretching)][24] and chrome yellow was detected. Additionally, in sample F409 the yellow-white-blue regions revealed the presence of chrome yellow, lead white, and Prussian blue, $Fe_4[Fe(CN)_6]_3$, while the green-blue crystals showed the presence of emerald green, $Cu(C_2H_3O_2)_2 \cdot 3Cu(AsO_2)_2$; there are no indications of the presence of viridian grains.

Elemental Distributions and Characterization of the Brown Altered Layers. The μ-XRF maps of sample F409 show that both Pb and Cr appear as main constituents of the yellow layer (Figure 3A), although the surface appears to be somewhat depleted in Cr and richer in S. In sample F293 on the other hand, only Pb is apparent as the main metallic constituent of the yellow paint, while smaller Cr-rich grains are visible in the yellow area (Figure 4A).

On both samples, the Raman spectra from the brown patina show an intense fluorescence signal, likely due to the presence of (degraded) organic material. In the dark layer of sample F409 (Figure 3B), the μ-XRF maps show the presence of Ca and Ba, sometimes associated with S (Figure 3A), suggesting the presence of $CaCO_3$, (chalk) $CaSO_4$ (gypsum) and/or $BaSO_4$ (barite) grains. While the intense fluorescence background signal from organic material does not permit their direct identification from the Raman spectra, we consider the assumption about the presence of chalk, gypsum, and barite to be reasonable, since they were commonly used as extenders of different paints. Raman spectroscopy and FTIR reflection analysis of the white, Ca-rich grains located in the brown layer, allowed their identification as $CaCO_3$ (signal at 1084 cm^{-1}, CO_3^{2-} symmetric stretching,[25] Figure 2A). The Ba- and S-rich grain indicated in Figure 3A was examined in more detail by means of μ-XANES (Figure 5).

In both brown layers, it is possible to observe Al, Si, K, and Ca (Figures 3B,C and 4B,C), and by means of FTIR, these elements could be shown to be associated with aluminum silicate com-

dx.doi.org/10.1021/ac1025122 |*Anal. Chem.* XXXX, XXX, 000–000

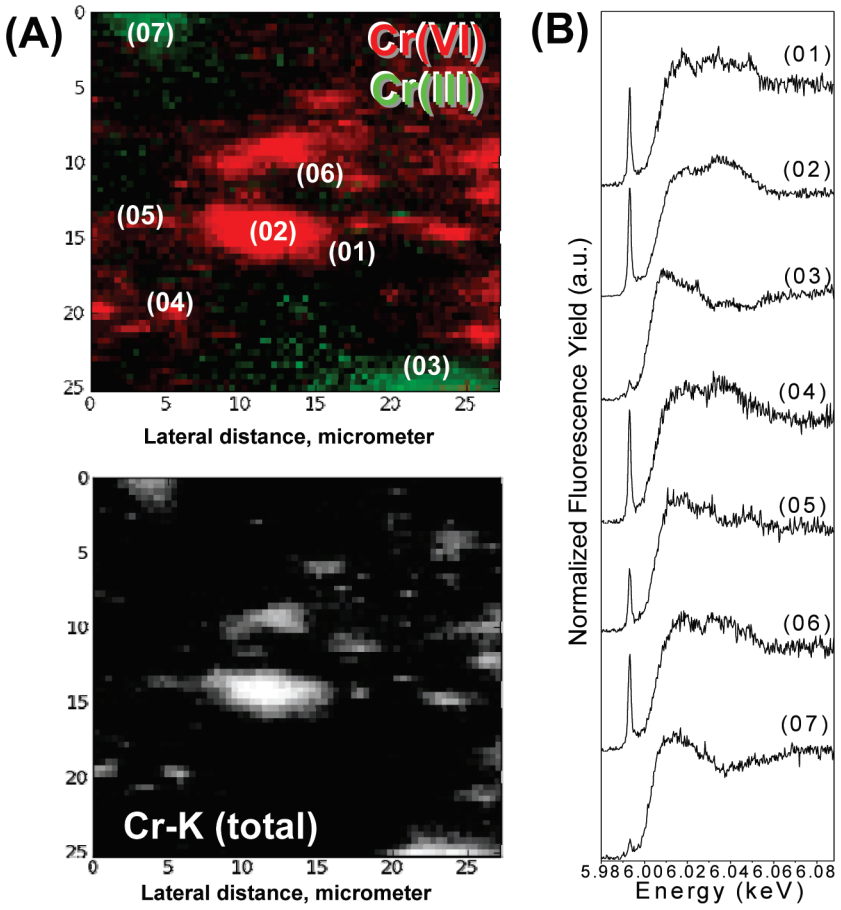

Figure 6. Panel A: composite images of chemical state map of Cr(VI) and Cr(III) and Cr distribution obtained by μ-XRF of paint sample F293. Map size: 25 × 28 μm^2; pixel size: 0.4 × 0.4 μm^2; dwell time: 0.3 s. The area on which was recorded the map is shown in Figure 4A and is indicated by a yellow rectangle. Panel B: Cr K-edge XANES spectra for paint sample F293. Measuring positions are indicated in the top picture shown in panel A.

pounds (such as kaolin). These compounds are either impurities of the pigment itself[1,2] and/or of the organic binder (in which they can be used as plasticisers) or are due to dust, deposited on the paint surface.[26,27]

In sample F293 (Figure 4A), the presence of sulfur, sometimes associated with Pb suggests the presence of $PbSO_4$; this is confirmed by μ-FTIR spectroscopy. In both samples also the diffuse presence of Cl can be observed. The black grains are carbon black (broad Raman bands at 1598 and 1348 cm^{-1}, Figure 2B).

Local Cr-Speciation Measurements and Chemical State Mapping. XANES measurements were performed inside a number of selected areas of samples F409 and F293, such as those indicated in Figures 3A and 4A. As demonstrated by a clear decrease of the intensity of the Cr pre-edge peak at 5.993 keV and the shift of the absorption edge toward lower energies, reduced Cr was observed in specific locations. In sample F409, the areas rich in Ba+S and in aluminum silicate compounds featured Cr(III) compounds; the results of the XANES line-scan analysis of a Ba, S-rich grain are summarized in Figure 5. In sample F293, Cr(III) was found to be present at the interface between the yellow-white paint and the brown coating, as shown in Figure 6.

The XANES line-scan through the Ba,S-rich grain was executed with a step size of 0.4 μm. In the surrounding yellow paint, on locations where no Ba is present, XANES spectra similar to that of $PbCrO_4$ are obtained (Figure 5B); on the other hand, in the positions rich in Ba and S, XANES spectra are observed that can be well described by a linear combination of the reference spectra of $Cr_2O_3 \cdot 2H_2O$ and $PbCrO_4$, roughly in a 60:30 ratio (see Figure 5C for an example of a fitting result). The variation of the $Cr_2O_3 \cdot 2H_2O$:$PbCrO_4$ ratio along the line is shown in Figure 5D. The species-specific maps of Figure 5A confirm that Cr(III) species are concentrated in the Ba,S-rich area. In Figure 5B also the Cr−K edge XANES spectrum of unaged paint samples prepared from 1:1 and 1:2 mixtures of $PbCrO_4$ and $BaSO_4$ are shown. These do not show any sign of Cr-reduction.

In sample F293, XANES point measurements carried out at the surface of the yellow layer in the area, indicated in Figure 4A, reveal that in some positions, up to 100% of the Cr has been reduced to the Cr(III) state (Figure 6B, points 03 and 07) while in others, the XANES spectrum only reveals the presence of Cr(VI) (points 01, 02, 04, and 06) or shows a mixture of oxidation states to be present (point 05). The corresponding total Cr and chemical state maps (Figure 6A), obtained using the procedure detailed elsewhere,[18] reveal the patchy nature of the distribution of both Cr(III) and Cr(VI) throughout the scanned area.

Hypotheses about the Causes of the Cr-Reduction. On the basis of the previous study carried out on artificially aged mode samples,[18] only the model paint sample rich in lead sulfate and in which the lead chromate is present in a very fine-grained/amorphous form showed a significant darkening after the aging process. Paint in which $PbCrO_4$ is present in pure, crystalline

dx.doi.org/10.1021/ac1025122 |*Anal. Chem.* XXXX, XXX, 000–000

form did not show an appreciable darkening after the same treatment. Similar to the model sample rich in $PbSO_4$, also in paint samples F293 and F409, the reduction of Cr appears to be associated with the presence of (one or more) sulfate compounds. On first sight this appears illogical, as sulfates, containing sulfur in its most oxidized form, cannot serve as an electron source in a reaction in which chromates are reduced.

Nevertheless, according to the literature, the observed colocalization of the reduced Cr with $BaSO_4$ and/or silicate compounds in sample F409 may be explained by one of two different processes:

(a) Minerals and organic matter can act as catalysts, promoting in situ reduction of Cr(VI) accompanied by the oxidation of a suitable redox reaction partner; these reactions, depending on the pH, may involve the CrO_4^{2-}, $HCrO_4^-$ and/or H_2CrO_4 species and are favored under photochemical conditions.[28]

(b) Absorption/desorption processes on mineral surfaces of aluminum silicate classes, such as kaolinite $[Al_2Si_2O_5(OH)_4]$[29] or montmorillonite $[(Na,Ca)_{0,3}(Al,Mg)_2Si_4O_{10}(OH)_2 \cdot n(H_2O)]$ in acidic conditions and in the presence of sulfide ions,[28] can promote the reduction of Cr(VI). The oxidation of the sulfides then leads to the formation of sulfur species in several oxidation states (e.g., $S_2O_6^{2-}$, SO_3^{2-}, SO_4^{2-}, S^0, and polysulfides).[30]

Moreover, considering that often lithopone ($BaSO_4 \cdot ZnS$, an equimolar mixture of barium white and zinc white) was used as white pigment by artists of the 19th Century, the presence of small amounts of sulfide-containing compounds, such as ZnS (although not explicitly revealed by the XRF maps of Figures 3−6) may not be completely excluded either in the material studied. To date, however, there is no published evidence of its use by van Gogh. In case sulfides are indeed present, a possible redox reaction involving chromate ions can then be written as:

$$8CrO_4^{2-} + 20H^+ + 3S^{2-} \rightleftarrows 8Cr^{3+} + 20OH^- + 3SO_4^{2-}$$

in which electrons released by sulfur are used to reduce chromium. Even in the absence of sulfide species, some studies have demonstrated that is possible that S^{2-} ions can be produced in situ from sulfates, after which chromate ions could react with sulfides to regenerate sulfate. According to Plummer,[31] sulfide ions can be produced in a redox equilibrium involving $BaSO_4$:

$$BaSO_4 + CO_2 + H_2O + Ca^{2+} \rightleftarrows Ba^{2+} + CaCO_3 + H_2S + 2O_2$$

The reduction of chromates could therefore be promoted by small quantities of sulfides that are generated in situ by the interaction of sulfates (such as $BaSO_4$) with CO_2 in the presence of Ca ions.

An alternative possibility for the in situ formation of S^{2-} ions under anaerobic conditions is by the intervention of sulfate-reducing bacteria (SRB).[32] This process is in general coupled with the oxidation of organic matter (a) or of H_2 (b), as shown by the following reactions:[33]

$$SO_4^{2-} + 2CH_2O \rightarrow H_2S + 2HCO_3^- \quad (a)$$

$$SO_4^{2-} + 4H_2 + 2H^+ \rightarrow H_2S + 4H_2O \quad (b)$$

CONCLUSIONS

In the present work, a combination of synchrotron radiation based X-ray techniques, μ-XRF and μ-XANES, and more conventional spectroscopic methods was employed to investigate two paint cross sections taken from paintings by Vincent van Gogh, in which pigment alteration was suspected. The results of this second part of the study agree with the observations derived from the previous analyses (part 1 of this study) on aged model samples, indicating that also on paintings the alteration of yellow $PbCrO_4$ may be associated with a reduction of the original Cr(VI) to Cr(III) and that sulfate anions likely play a key role in this alteration process.

In both microsamples, at the exposed surface of $PbCrO_4$-containing paint layers, the presence of reduced Cr was observed, especially in locations where either Ba+S or other components are present. These compounds may act as catalysts for the reduction of the chromate ions. At present we assume that especially sulfide anions, that may be present in the form of the white pigment lithopone ($BaSO_4 \cdot ZnS$) or that may be generated in situ from $BaSO_4$ and/or other sulfates, may play an essential role in the redox transformation. To prove the latter aspect of the degradation mechanism, a systematic additional effort is under way, involving, among others, the study of several (un)aged synthetized coprecipitates of lead chromate-sulfate (containing CrO_4^{2-} and SO_4^{2-} in different percentage ratio concentrations), sometimes mixed with $BaSO_4$. The presence of sulfate anions during Cr(VI)-reduction seems to play a key role, confirming our first observations. The recently aged model samples show a clear darkening that is particularly significant for those containing greater amounts of sulfate. We intend to discuss the results of these investigations, involving Cr-edge XANES and EELS analyses coupled to XANES measurements at the S K-edge, in part 3 of this series of papers. In the current study we relied on the analysis of two paint samples that were taken for earlier studies. In order to validate the conclusions drawn so far and for further comparison with the model work (part 3), it will be highly relevant to study a more representative set of lead chromate paint samples from van Gogh's oeuvre and his contemporaries featuring, e.g., different CrO_4^{2-}:SO_4^{2-} ratio's (part 4).

AUTHOR INFORMATION

Corresponding Author

*Tel: +32 3 820 2373. Fax: +32 3 820 23 76. E-mail: koen.janssens@ua.ac.be.

ACKNOWLEDGMENT

This research was funded by grants from ESRF (experiment EC-504) and by HASYLAB (experiments II-20080130 EC and II-20070157 EC) and was supported by the Interuniversity Attraction Poles Programme−Belgian Science Policy (IUAP VI/16). The text also presents results of GOA "XANES meets ELNES" (Research Fund University of Antwerp, Belgium) and from FWO (Brussels, Belgium) project nos. G.0103.04, G.0689.06, and G.0704.08. The staff of the Van Gogh Museum, Amsterdam, is acknowledged for their agreeable cooperation and for the authorization to publish the images of the paintings in this article. L.M. was financially supported by the Erasmus Placement in the framework of Lifelong Learning Programme (A.Y. 2009-2010). The EU Community's FP7 Research Infrastructures program under the CHARISMA Project (Grant Agreement 228330) is also acknowledged.

REFERENCES

(1) Kühn, H.; Curran, M. . In *Artists' Pigments: a handbook of their history and characteristics*; Feller, R. L., Ed.; Cambridge University Press: New York, 1986; Vol. 1, pp 187−200.

(2) Eastaugh, N.; Walsh, V.; Chaplin, T.; Siddall, R. *The Pigment Compendium [CD-ROM]*; Elsevier: New York, 2004.

401 (3) Kirby, J.; Stonor, K.; Roy, A.; Burnstock, A.; Grout, R.; White, R. *Natl. Gallery Tech. Bull.* **2003**, *24*, 4–37.
403 (4) Townsend, J. H. *Stud. Conserv.* **1993**, *38*, 231–254.
404 (5) Cove, S. . In *Constable*; Parris, L.; Fleming-Williams, I., Eds.; Tate
405 Gallery: London, 1991; pp 493−518.
406 (6) Butler, M. H. *Bull. Am. Inst. Conserv. Hist. Art. Works* **1973**, *13*,
407 77–85.
408 (7) Bomford, D.; Kirby, J.; Leighton, J.; Roy, A. *Art in the Making:*
409 *Impressionism*; London: National Gallery Publications, 1990; p 158.
410 (8) Van der Snickt, G.; Janssens, K.; Schalm, O.; Aibéo, C.; Kloust,
411 H.; Alfeld, M. *X-Ray Spectrom.* **2010**, *39*, 103–111.
412 (9) Hendriks, E. In *New Views on Van Gogh's Development in*
413 *Antwerp en Paris: An Integrated Art Historical and Technical Study of*
414 *His Paintings in the Van Gogh Museum*; Hendriks, E., Van Tilborgh, L.,
415 Eds.; University of Amsterdam: Amsterdam, The Netherlands, 2006; pp
416 149−150.
417 (10) Cole, R. J. *Paint Res. Assoc. Tech. Pap.* **1955**, *199*, 1–62.
418 (11) Watson, V.; Clay, H. F. *J. Oil Colour Chem. Assoc.* **1955**, *38*,
419 167–177.
420 (12) Eibner, A. *Chem. Ztg.* **1911**, *82*, 753–755.
421 (13) Haug, R. *Dtsch. Farben-Z.* **1951**, *5*, 343–348.
422 (14) Erkens, L. J. H.; Hamers, H.; Hermans, R. J. M.; Claeys, E.;
423 Bijnens, M. *Surf. Coat. Int., Part B* **2001**, *84*, 1969–1976.
424 (15) Bronwyn, L.; Burnstock, A.; Jones, C.; Hallebeek, P.; Boon, J. J.;
425 Keune, K. In *Preprints of the 14th Triennial Meeting of ICOM Committee*
426 *for Conservation*; The Hague, September 2005, London: James & James,
427 2005, Vol. *2*, pp 803−813.
428 (16) Van der Snickt, G.; Dik, J.; Cotte, M.; Janssens, K.; Jaroszewicz,
429 J.; De Nolf, W.; Groenewegen, J.; Van der Loeff, L. *Anal. Chem.* **2009**, *7*,
430 2600–2610.
431 (17) Casadio, F.; Xie, S.; Rukes, S. C.; Myers, B.; Gray, K. A.; Warta,
432 R.; Fiedler, I. *Anal. Bioanal. Chem.* **2010**, DOI: 10.1007/s00216-010-
433 4264-9.
434 (18) Monico, L.; Van der Snickt, G.; Janssens, K.; De Nolf, W.;
435 Miliani, C.; Verbeeck, J.; Tian, H.; Tan, H.; Dik, J.; Radepont, M.; Cotte,
436 M. *Anal. Chem.* **2010,** DOI: 10.1021/ac102424h.
437 (19) Cotte, M.; Welcomme, E.; Solé, V. A.; Salomé, M.; Menu, M.;
438 Walter, P.; Susini, J. *Anal. Chem.* **2007**, *79*, 6988–6994.
439 (20) Susini, J.; Salomè, M.; Fayard, B.; Ortega, R.; Kaulich, B. *Surf.*
440 *Rev. Lett.* **2002**, *9*, 203–211.
441 (21) Solé, V. A.; Papillon, E.; Cotte, M.; Walter, P.; Susini, J.
442 *Spectrochim. Acta, Part B* **2007**, *62*, 63–68.
443 (22) Ravel, B.; Newville, M. *J. Synchrotron Rad.* **2005**, *12*, 537–541.
444 (23) Frost, R. L. *J. Raman Spectrosc.* **2004**, *35*, 153–158.
445 (24) Brooker, M. H.; Sunder, S.; Taylor, P.; Lopata, V. J. *Can. J.*
446 *Chem.* **1983**, *61*, 494–502.
447 (25) Edwards, H. G. M.; Jorge Villar, S. E.; Jehlicka, J.; Munshi, T.
448 *Spectrochim. Acta, Part A* **2005**, *61*, 2273–2280.
449 (26) Gysels, K.; Delalieux, F.; Deutsch, F.; Van Grieken, R.; Camuffo,
450 D.; Bernardi, A.; Sturaro, G.; Busse, H. J.; Wieser, M. *J. Cult. Herit.* **2004**,
451 *5*, 221–230.
452 (27) De Bock, L. A.; Van Grieken, R.; Camuffo, D.; Grime, G. W.
453 *Environ. Sci. Technol.* **1996**, *30*, 3341–3350.
454 (28) Tzou, Y. M.; Loeppert, R. H.; Wang, M. *J. Environ. Qual.* **2003**,
455 *32*, 2076–2084.
456 (29) Zachara, J. M.; Cowan, C. E.; Schmidt, R. L.; Ainsworth, C. C.
457 *Clays Clay Miner.* **1988**, *36*, 317–326.
458 (30) Kim, C.; Zhou, Q.; Deng, B.; Thornton, E. C.; Xu, H. *Environ.*
459 *Sci. Technol.* **2001**, *35*, 2219–2225.
460 (31) Plummer, L. N. *Econ. Geol.* **1971**, *66*, 252–258.
461 (32) Somasundaram, V.; Philip, L.; Murty Bhallamudi, S. *J. Hazard.*
462 *Mater.* **2009**, *172*, 606–617.
463 (33) Shen, Y.; Buick, R. *Earth-Sci. Rev.* **2004**, *64*, 243–272.